Stability and degradation of organic photovoltaics fabricated, aged, and characterized by the ISOS 3 inter-laboratory collaboration

David M. Tanenbaum*[a,b], Martin Hermenau[c], Eszter Voroshazi[d], Matthew T. Lloyd[e], Yulia Galagan[f], Birger Zimmermann[g], Markus Hösel[a], Henrik F. Dam[a], Mikkel Jørgensen[a], Suren Gevorgyan[a], Suleyman Kudret[h], Wouter Maes[h], Laurence Lutsen[h], Dirk Vanderzande[h], Uli Würfel[g], Ronn Andriessen[f], Roland Rösch[i], Harald Hoppe[i], Monica Lira-Cantu[j], Gerardo Teran-Escobar[j], Aurélie Dupuis[k], Pierre-Olivier Bussière[k], Agnès Rivaton[k], Gülşah Y. Uzunoğlu[l], David Germack[m], Birgitta Andreasen[a], Morten V. Madsen[a], Kion Norrman[a], Eva Bundgaard[a] and Frederik C. Krebs[a]

[a] *Department of Energy Conversion and Storage, Technical University of Denmark, Frederiksborgvej 399, DK-4000 Roskilde, Denmark.*
[b] *Department of Physics and Astronomy, Pomona College, Claremont, CA 91711, USA.*
[c] *Arbeitsgruppe Organische Solarzellen (OSOL),Institut für Angewandte Photophysik,Technische Universität Dresden, 01062 Dresden, Germany,*
[d] *imec, Kapeldreef 75, 3000 Leuven, Belgium and Katholieke Universiteit Leuven, ESAT, Kasteelpark Arenberg 10, 3000 Leuven, Belgium.*
[e] *National Renewable Energy Laboratory, Golden, CO 80401, USA.*
[f] *Holst Centre, High Tech Campus 31, 5656 AE Eindhoven, The Netherlands.*
[g] *Fraunhofer Institute for Solar Energy Systems ISE, Heidenhofstrasse 2, D-79110 Freiburg, Germany.*
[h] *Hasselt University, Campus, Agoralaan 1, Building D, WET/OBPC, B-3590 Diepenbeek, Belgium.*
[i] *Institute of Physics, Ilmenau University of Technology, Weimarer Str. 32, 98693 Ilmenau, Germany*
[j] *Centre d'Investigació en Nanociència i Nanotecnologia (CIN2, CSIC), Laboratory of Nanostructured Materials for Photovoltaic Energy, ETSE, Campus UAB, Edifici Q, 2nd Floor, E-08193, Bellaterra (Barcelona), Spain.*
[k] *Clermont Université, Université Blaise Pascal, Laboratorie de Photochemie, Moléculaire et Macromoléculaire (LPMM), BP10448 Clermont-Ferrand, France and CNRS, UMR6505, LPMM, F-63177 Aubière, France.*
[l] *TÜBİTAK National Metrology Institute (UME),Photonic and Electronic Sensors Laboratory, P.O. Box 54, 41470, Gebze, Kocaeli, TURKEY.*
[m] *Condensed Matter Physics, Brookhaven National Lab, Building 510B Upton, NY, 11973.*

Abstract

Seven distinct sets ($n \geq 12$) of state of the art organic photovoltaic devices were prepared by leading research laboratories in a collaboration planned at the Third International Summit on Organic Photovoltaic Stability (ISOS-3). All devices were shipped to DTU and characterized simultaneously up to 1830 h in accordance with established ISOS-3 protocols under three distinct illumination conditions: accelerated full sun simulation; low level indoor fluorescent lighting; and dark storage with daily measurement under full sun simulation. Three nominally identical devices were used in each experiment both to provide an assessment of the homogeneity of the samples and to distribute samples for a variety of post soaking analytical measurements at six distinct laboratories enabling comparison at various stages in the degradation of the devices. Characterization includes current-voltage curves, light beam induced current (LBIC) imaging, dark lock-in thermography (DLIT), photoluminescence (PL), electroluminescence (EL), *in situ* incident photon-to-electron conversion efficiency (IPCE), time of flight secondary ion mass spectrometry (TOF-SIMS), cross sectional electron microscopy (SEM), UV visible spectroscopy, fluorescence microscopy, and atomic force microscopy (AFM). Over 100 devices with more than 300 cells were used in the study. We present here design of the device sets, results both on individual devices and uniformity of device sets from the wide range of characterization methods applied at different stages of aging under the three illumination conditions. We will discuss how these data can help elucidate the degradation mechanisms as well as the benefits and challenges associated with the unprecedented size of the collaboration.

Keywords: Organic Photovoltaics Stability, Organic Photovoltaics Degradation Mechanisms, Organic Photovoltaics Characterization

1. INTRODUCTION

Organic photovoltaics have advanced steadily over the past decade. During this time, impressive progress has been reported on power conversion efficiency (*PCE*), scalable processing technology, characterization methods, chemical and physical origins of device degradation, and approaches to improve device stability by introduction of new materials and architectures including UV filters and protective encapsulation schemes. The collaboration in this report is the result of the collective discussions at the first three International Summits on Organic Photovoltaic Stability (ISOS-1-3) where scientists working on the development and manufacture of organic solar cells met to exchange experiences and discuss methods of manufacture, materials and measuring techniques. Here we present the stability data and detailed characterization for seven distinct sets of OPV devices simultaneously illuminated and characterized in one of three

Organic Photovoltaics XIII, edited by Zakya H. Kafafi, Christoph J. Brabec, Paul A. Lane,
Proc. of SPIE Vol. 8477, 847704 · © 2012 SPIE · CCC code: 0277-786X/12/$18 · doi: 10.1117/12.930451

distinct environments at Risø DTU: accelerated full sun simulation; low level indoor fluorescent lighting; and dark storage with daily measurement under full sun simulation. Characterization includes current-voltage curves, light beam induced current (LBIC) imaging, dark lock-in thermography (DLIT), photoluminescence (PL), electroluminescence (EL), *in situ* incident photon-to-electron conversion efficiency (IPCE), time of flight secondary ion mass spectrometry (TOF-SIMS), cross sectional electron microscopy (SEM), UV visible spectroscopy, fluorescence microscopy, and atomic force microscopy (AFM). The cells tested represent a wide range of state of the art technologies including both normal and inverted device types. Encapsulations range from open faced to full glass with epoxy seals and internal getter materials. Active materials include evaporated small molecule films as well as formulations with Poly(3-hexylthio-phene) (P3HT) or copolymers based on P3HT and [6,6]-phenyl C61-butyric acid methylester (PCBM) in bulk mixtures. A range of materials and geometries are used as electrodes and hole and electron transport layers (HTL and ETL). Two devices are free of indium tin oxide (ITO). Processing methods included spin coating, thermal evaporation, ink jet printing, slot die coating, and screen printing. Cells were fabricated in a range of environmental conditions with both manual and fully automated processing tools. Both rigid glass and flexible PET substrates were used producing cells with active areas from 0.064 - 4.9 cm^2. Details of the specific device structures and fabrication process have been published in our previous publication.[1]

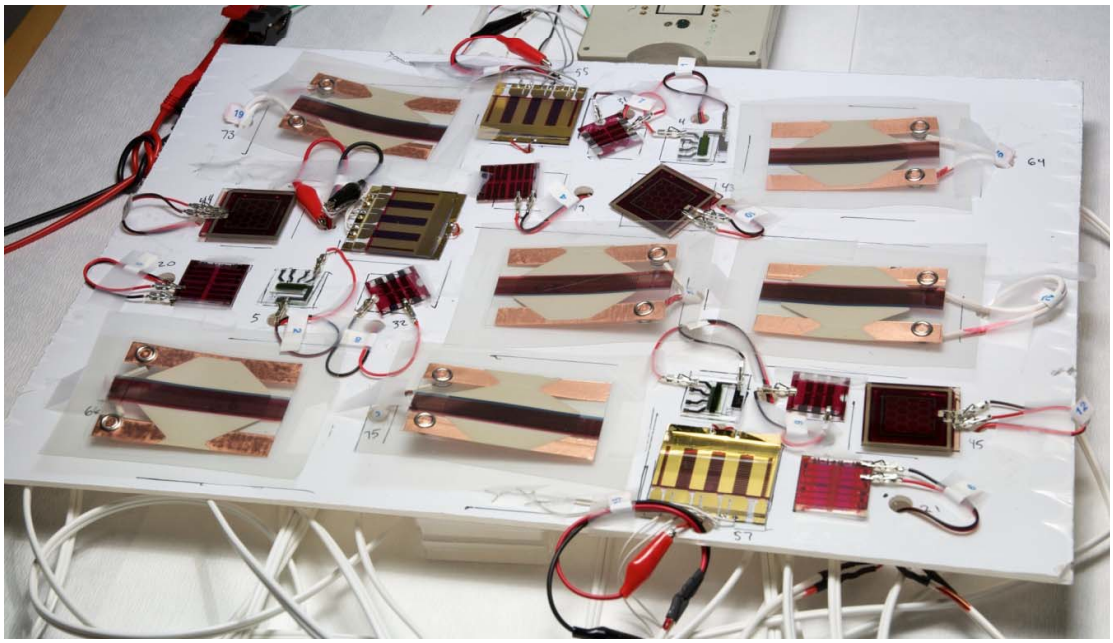

Figure 1. A series of different state of the art OPV devices during IV characterization under 1 sun illumination. In this case 21 devices are measured simultaneously, 3 of each of the 7 device types.

Cells were selected for analysis at 4 stages of degradation corresponding roughly to T100 (initial characterization), T80 (when the PCE declines to 80% of its peak value), T50, and T10 from each of the three illumination environments. Non destructive analysis includes imaging by light beam induced current (LBIC), dark lock-in thermography (DLIT) , electroluminescence (EL) and photoluminescence (PL). Each analysis technique is applied uniformly by a single research group to all the cells in the study. *In situ*-Incident Photon to Charge Carrier Efficiency (IPCE) are recorded as well. Cells were then submitted for destructive testing including: time of flight secondary ion mass spectroscopy (TOF-SIMS); cross sectional scanning electron microscopy (SEM) with energy dispersive X-ray spectroscopy (EDS); optical and fluorescence microscopy; absorbance spectroscopy; atomic force microscopy (AFM); and IR spectroscopy. As a result of the collaboration, these devices are among the most thoroughly characterized OPV cells in any study. Such investigations are truly beyond the capability and expertise of any one research laboratory, and the full data analysis of the range of devices should open new insights in the optimization of OPVs and the variety of mechanisms by which they degrade.

2. STABILITY TESTING

2.1 Electrical Characterization

All illumination sources were characterized with both a pyranometer (Kipp & Zonen, CM 4) and a calibrated fiber optic spectrometer (Avantes, Avaspec). Room humidity was uncontrolled ambient, and temperature was monitored periodically via thermocouple on the back of the devices. Due to the large number of devices and geometries, no masks were applied in this study. Active areas were defined by electrode geometries provided by cell manufacturers, and no spectral mismatch factors were applied. There are several complexities when setting up automated measurements on so many different device types. Some devices had electrical connectors to the thin film electrodes, while other devices had exposed metal contact pads. In most cases subminiature alligator clips (Hirschmann) were employed. This works best with an additional layer of silver paint or epoxy to minimize the scratching of the thin evaporated metal electrodes over time. Fully automated *IV* characterization was performed on devices under illumination at either 10 or 15 minute intervals with a pair of custom built multiplexing systems, each controlling a sourcemeter (Keithley 2400) and a 40x2 channel switching relay matrix (Keithley 2700) under computer control. Devices were open circuit between measurements.

2.2 Accelerated Full Sun Simulation Testing

The accelerated full sun simulation was run AM1.5G (1000 W m-2, 85 ± 5° C, metal halide lamp, KHS Solar Constant 1200) in accordance with ISOS-L-1. A wide range of performance is observed as seen in Figure 2. Fully encapsulated small molecule cells prepared by IAPP showed no discernable degradation in performance. In contrast to devices with wet processing of layers, in the other devices, the IAPP devices all layers are deposited via thermal evaporation in vacuum. This makes these devices thermally stable, even in our accelerated full sun environment. They are also the only devices encapsulated with a getter giving them the best protection from oxygen and water infiltration when properly sealed. In comparison, the IMEC devices have no encapsulation, and show a significant initial decay, but then stabilize remarkably well. While these devices are based on P3HT:PCBM active layers, the IMEC devices contain an evaporated MoO_3 hole transport layer (HTL) rather than using PEDOT:PSS which is common to the other devices in the study.

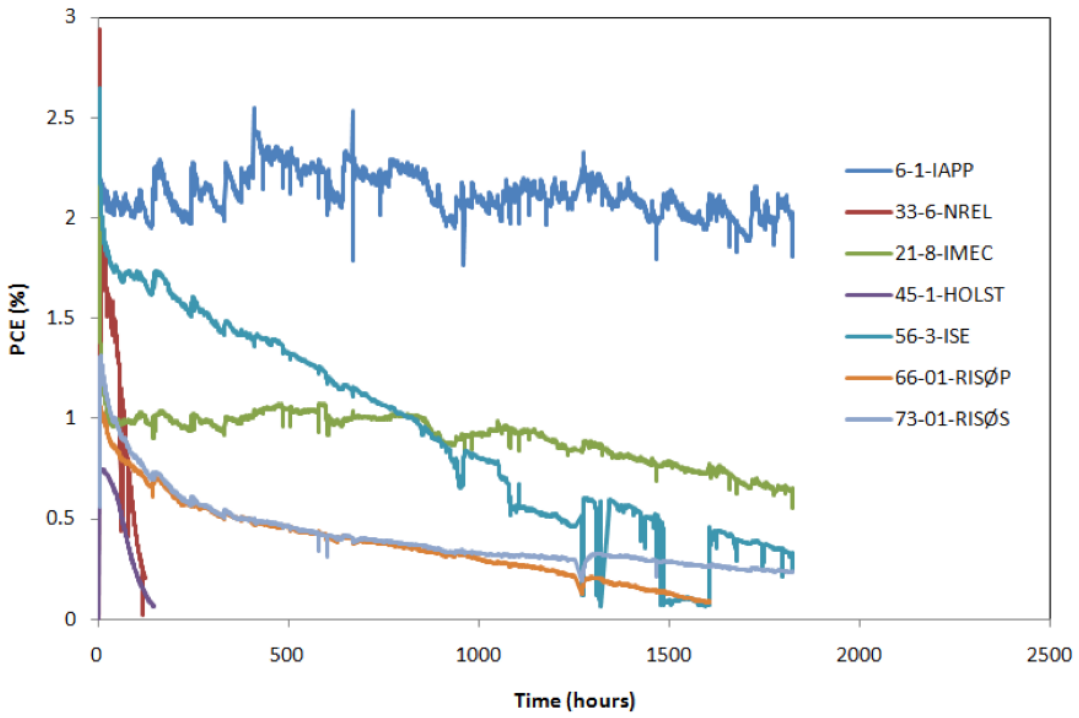

Figure 2. A plot of photovoltaic conversion efficiency (PCE) over time under 1 sun illumination for a series of different state of the art OPV devices. Figure taken from reference 1.

2.3 Low Level Indoor Fluorescent Light Testing

The low level indoor low light test was run under a bank of fluorescent lamps (100 W/m^2, Osram FQ Lumilux HO, T~45° C) in accordance with ISOS-Low Light-1 standards. When comparing with the accelerated full sun conditions, it is clear that the stability is much better for most of the devices. The HOLST and ISE (Fraunhofer) devices are particularly impressive. Both of these devices are ITO-free and employ fine metal current collecting grids with PEDOT:PSS for the HTL layer. In both cases it is observed at the home laboratories that these devices have similar stability even under full sun illumination if the sample temperatures are kept below 50˚C, and thus the degradation seen in the accelerated full sun simulation is likely due to a thermally driven instability, which does not come into play under low light conditions.

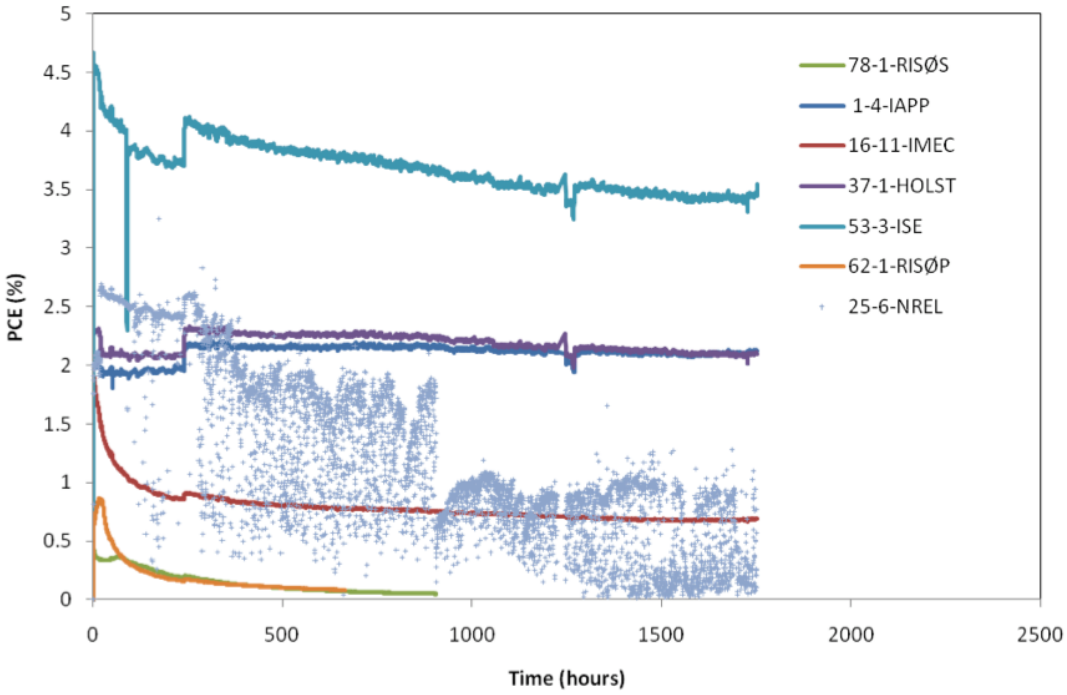

Figure 3. A plot of photovoltaic conversion efficiency (PCE) over time under low level indoor fluorescent illumination for a series of different state of the art OPV devices. Figure taken from reference 1.

2.4 Dark Storage with Daily Full Sun Characterization

The dark storage data are similar to the low level indoor fluorescent data, with the unencapsulated IMEC and NREL devices showing the most significant initial degradation. The RISØS and RISOØP devices are the exception in this case, as their stability is much better than under the low level fluorescent conditions, where they performed particularly poorly. This can be attributed to the fact that there is not enough UV light present in the low level fluorescent condition to activate the ZnO electron transport layer in these devices which have a UV filter incorporated in their structure. Under dark storage with daily full sun testing from a metal halide lamp, these devices demonstrate a significant improvement in stability as was reported in our previous publication.[1]

3. CHARACTERIZATION AND ANALYSIS

3.1 Protocols

Under all three illumination conditions, devices were pulled from the experiment for detailed imaging and destructive analysis at 4 stages of degradation corresponding roughly to T100 (initial characterization), T80, T50, and T10. This

involves sending samples to six different laboratories in six countries. In the case of destructive analysis of encapsulated samples, the encapsulation was opened in an oxygen free glove box, and samples were packed under dry nitrogen in sealed containers to be opened in the analytical laboratories. In addition, one set of cells was "cycled" from the full sun simulation only for nondestructive imaging and IPCE analysis, and then returned to the stability test, enabling specific cells to be imaged at multiple stages of degradation. Those cycle cells are the focus of a recently submitted publication.[2]

3.2 Non Destructive Spatial Imaging Data

More than 50 different nondestructive spatial images were acquired for each of the 7 cell types. An example of these images is shown for the Fraunhofer ISE devices in Figure 4. The DLIT images show milli-Kelvin (mK) variations in temperature during the biasing of the devices without illumination. The reverse image highlights short circuits in the devices while the forward images highlight charge transport. In contrast the LBIC images show spatial maps of pico-ampere photocurrents created by generation of carriers excited by a rapidly scanned laser over the active area of the devices and reveals inhomogeneity in the efficiency of the devices. The EL images show the spatial map of the very weak luminescence when the OPVs are driven under forward bias, similar to OLEDs. EL requires locally functioning electrode-active layer interfaces reveals failures of this sensitive part of the device with very high resolution. Conversely, PL does not require working electrodes, and the true PL signal is largely a reflection of the quality of the bulk heterojunction morphology in the active layer, although despite application of cutoff filters reflected excitation light competes with the true photoluminescence signal.

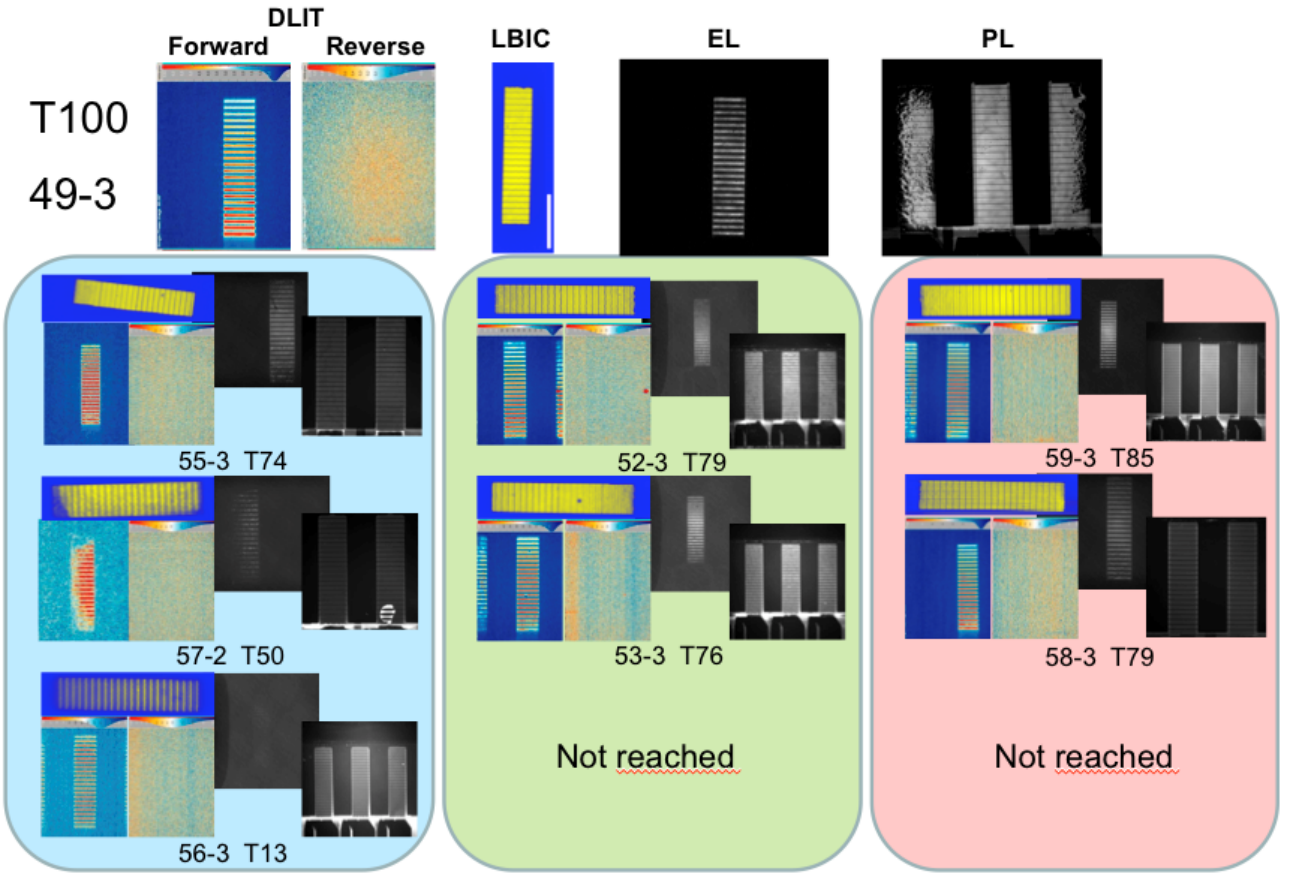

Figure 4. A series of different imaging techniques applied to OPV devices made by Fraunhofer ISE. Each technique provides distinct but complementary information. The top row is a cell at T100, shortly after its manufacture. The blue, green, and red regions show cells imaged after aging under different illumination conditions, full sun, low light, and dark storage respectively. Full IV curves and IPCE measurements were recorded at each stage as well followed by destructive analysis methods.

Several critical features can be seen in the images in Figure 4. The DLIT images of sample 52-3 show a short in the right most solar cell. The DLIT, LBIC, and EL images show a defect in sample 53-3, suggesting that delamination may have occurred in this solar cell, which does not appear in the PL signal. In contrast the PL signal in device 49 can reveal serious degradation of the adjacent solar cells highlighting an edge diffusion degradation mechanism. Similar degradation appears to happen to the electrode interfaces in 57-2 as detected by DLIT and LBIC images.

3.3 Incident Photon to Charge Carrier Efficiency (IPCE) and *in-situ* IPCE

Following spatial imaging, IPCE and *in-situ* IPCE were performed to analyze the different degradation paths observed on the devices. The IPCE signal is the number of charge carriers collected by the solar cell relative to the number of photons of a given energy adsorbed by the device. The IPCE spectrum has specific peaks associated with specific materials in the device structure. Changes in specific wavelengths of the IPCE spectra correlate with changes in the corresponding materials in the cell, thus helping identify degradation mechanisms. *In-situ* IPCE can be performed by varying the concentration of cell environment between ambient air and dry nitrogen in sealed chamber. Changes in the spectra with exposure to ambient oxygen and water highlight materials that are more susceptible to degradation due to the ambient atmosphere.

Figure 5 shows changes in the normalized IPCE curves for the IMEC devices as they degrade under the accelerated full sun illumination. The IPCE analysis reveals that the causes of degradation are related to the oxide electrodes, ZnO and MoO_3, as indicated by the steady decrease of the peaks below 400 nm. Another important factor is the degradation of the IPCE peaks that correspond to the P3HT at 560 nm and 600 nm (with respect to the reference device) which translates to a decrease of the current density of the IV curves. The change of the maximum IPCE peak with time, due to the decrease of the maximum IPCE peak at 575 nm (reference) and the emerging of a peak at 525 nm, indicate that the [P3HT-Oxygen] charge transfer complex disappears with longer irradiation times due to degradation of the P3HT.[3]

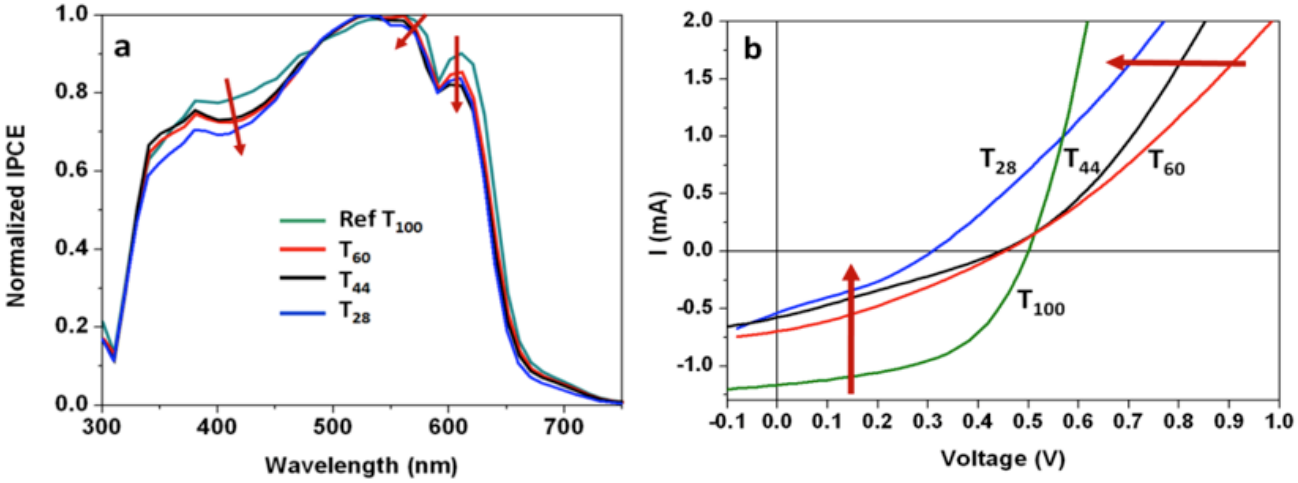

Figure 5. Un-encapsulated IMEC solar cells under the full sun stability test. a) PCE vs. time, b) normalized IPCE analysis and c) IV curves. Data corresponds to the full sun stabilization test at T_{100}, T_{60}, T_{44} and T_{28}.

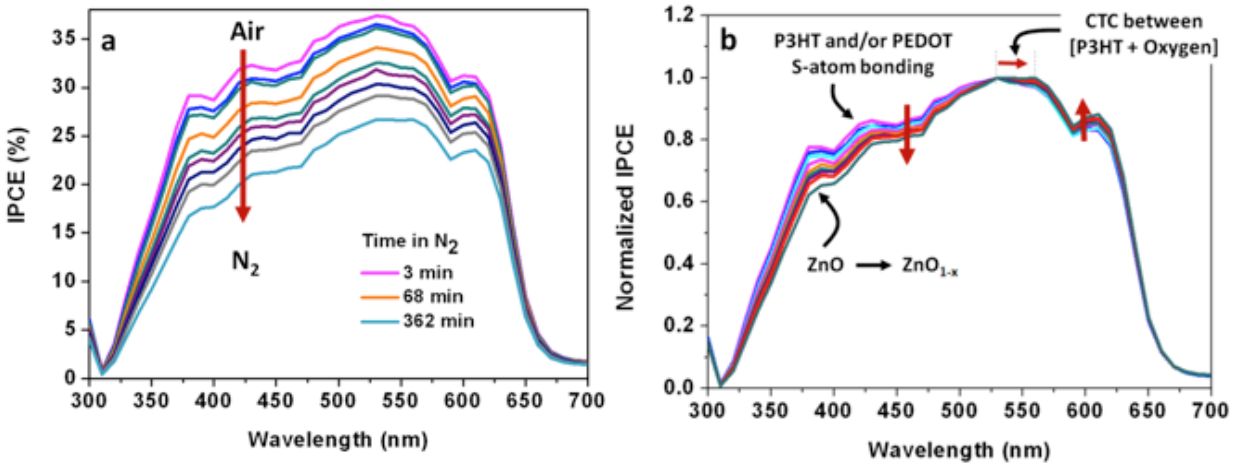

Figure 6. *in-situ* IPCE analysis of an NREL device (left) and the normalized IPCE spectra (right).

Figure 6 shows an example of the *in-situ* IPCE analysis applied to the unencapsulated NREL device. The wavelength region above 500 nm corresponds to the P3HT polymer; the shift observed for the peak at 530 nm towards 560 nm is well known to be due to the formation of a reversible charge transfer complex between organic semiconductors in the active layer (C_{60} or P3HT) and oxygen, while the decrease of the peak at 360 nm is associated with changes in the ZnO.[3]

3.4 Preliminary TOF SIMS Analysis

Uptake of oxygen in the active layer can also be seen in the destructive TOF SIMS measurements. An example is shown in Figure 7 for the RISØP samples where the relative uptake of oxygen is plotted against the degradation in cell efficiency for samples pulled at different stages from the full sun illumination condition.

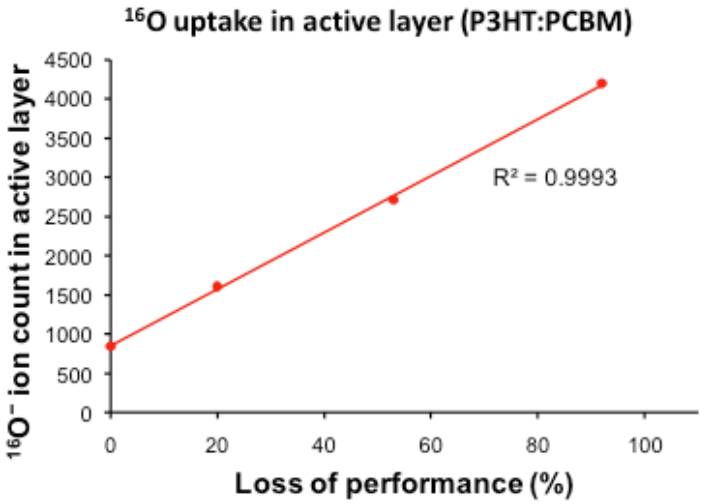

Figure 7. A strong correlation is observed between oxygen uptake and the loss of performance for the RISØP devices.

3.5 Optical Measurements: UV-Visable Absorption and Microfluorescence

In some samples the cathode could be removed by delamination and UV-vis absorption measurements could be made on the devices. In other cases this was only possible between the metal cathodes, but in those cases we see a clear difference between the material under the cathode and between cathodes. Figure 8 shows the UV-vis absorption of the RISØ cells under the cathode region at the same degradation levels as in the TOF SIMS experiments. In contrast no significant changes were observed in these devices in fluorescence imaging or AFM phase imaging.

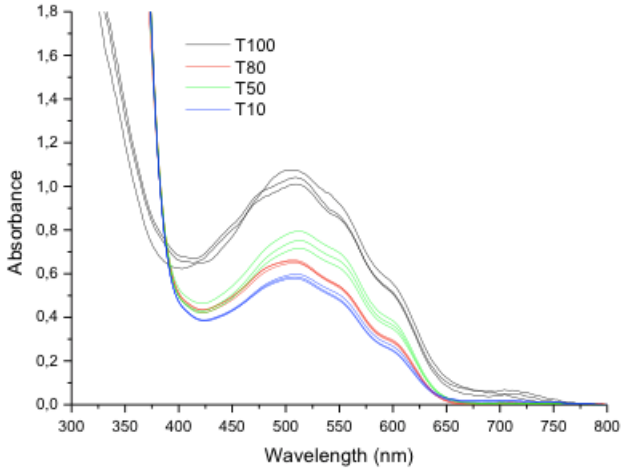

Figure 8. The RISØP devices display significant decrease in absorbance as the cells degrade.

In contrast, the Fraunhofer ISE devices showed no significant loss in absorbance under the cathodes as the cells degraded, but did show as significant increase in microfluorescence, as the quenching of the P3HT fluorescence by the PCBM became less efficient as seen in Figure 9.

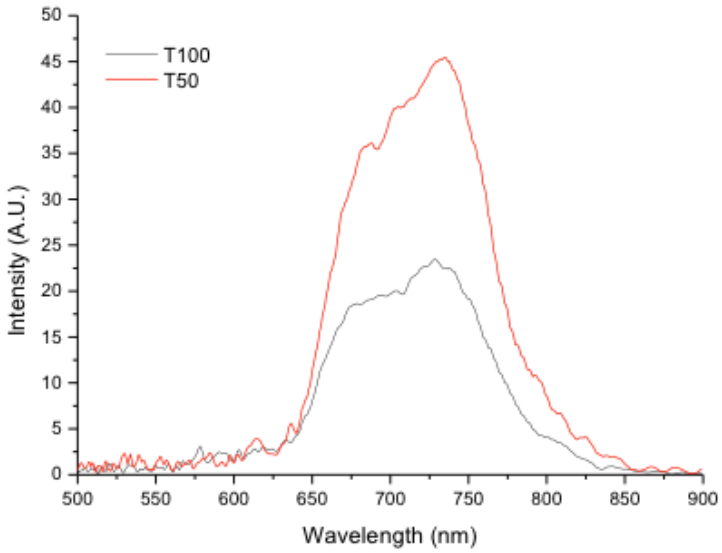

Figure 9. The ISE devices display significant increase in microfluorescence as the cells degrade.

The optical measurements demonstrate that there are significant changes in the active layer of the OPV cells as they degrade, but these changes are not uniform for the different devices, and may not be driving the degradation in performance.

4. CONCLUSIONS

The rapid progess of OPV technology makes it very difficult for any one laboratory to do everything well from materials chemistry to device architectures to fabrication methods to characterization. The ISOS inter-laboratory study has made reliable comparisons of devices aged uniformly under 3 standard illumination conditions from several different

independent laboratories with a wide range of analytical techniques. The unparalleled collaboration provided enhanced communication and active discussion about the primary mechanisms of device degradation in different types of state of the art devices.

It is quite clear that the degradation mechanisms are not the same for all the cell types, nor is it clear that only a single mechanism is responsible for the degradation of any one device type. The combination of different types of encapsulation, inverted and normal device structures, variation in electron and hole transport layer materials and active layer materials helps us to draw conclusions about the degradation of OPVs. Perhaps most promising is that both the imaging studies and the IPCE measurements suggest that much of the degradation is happening at the electrodes and their interfaces to the various layers of the devices, rather than in the organic semiconductors that comprise the active layers in the bulk heterojunctions. Several of the devices exhibited impressive performance, particularly in the low light condition, and have potential for use in full sun conditions with adequate cooling.

The benefits of the collaboration have been substantial to all the parties involved as well as to the research community at large. This should help seed new collaborations in the future.

REFERENCES

[1] D.M. Tanenbaum, M. Hermenau, E. Voroshazi, M.T. Lloyd, Y. Galagan, B. Zimmermann, M. Hösel, H.F. Dam, M. Jørgensen, S.A. Gevorgyan, S. Kudret, W. Maes, L. Lutsen, D. Vanderzande, U. Würfel, R. Andriessen, R. Rösch, H. Hoppe, M. Lira-Cantu, A. Rivaton, G.Y. Uzunoğlu, D. Germack, B. Andreasen, M.V. Madsen, K. Norrman, F.C. Krebs, *The ISOS-3 inter-laboratory collaboration focused on the stability of a variety of organic photovoltaic devices*., RSC Advances, 2 (2012) 882-893.

[2] R. Rosch, D.M. Tanenbaum, M. Jørgensen, M. Seeland, Maik Bärenklau, M. Hermenau, E. Voroshazi, M.T. Lloyd, Y. Galagan, B. Zimmermann, M. Hösel, H.F. Dam, S.A. Gevorgyan, S. Kudret, W. Maes, L. Lutsen, D. Vanderzande, U. Würfel, R. Andriessen, G. Teran-Escobar, M. Lira-Cantu, A. Rivaton, G.Y. Uzunoğlu, D. Germack, B. Andreasen, M.V. Madsen, K. Norrman, H. Hoppe, F.C. Krebs, *The ISOS-3 inter-laboratory collaboration- Investigation of the degradation mechanism of a variety of organic photovoltaic devices by combination of imaging techniques*., RSC Advances. In press, (2012).

[3] M. Lira-Cantu, G. Teran-Escobar, D.M. Tanenbaum, E. Voroshazi, M. Hermenau, K. Norrman, M.T. Lloyd, Y. Galagang, M.H. Birger Zimmermannh, Henrik F. Damb, Mikkel Jørgensen, Suren Gevorgyan, Laurence Lutsen, Dirk Vanderzande, Uli Würfel, Ronn Andriessen, Roland Rösch, Harald Hoppe, Agnès Rivaton, Gülşah Y. Uzunoğlu, David Germack, Birgitta Andreasen, Morten V. Madsen, Eva Bundgaard and Frederik C. Krebs, *On the stability of a variety of organic photovoltaic devices by IPCE and in-situ IPCE analyses - The ISOS-3 inter-laboratory collaboration*., In Preparation (2012).